THE JOURNAL OF PHYSICAL CHEMISTRY B

ARTICLE

pubs.acs.org/JPCB

# Molar Absorbance Coefficient of Pyrene Aggregates in Water Generated by a Poly(ethylene oxide) Capped at a Single End with Pyrene

Howard Siu and Jean Duhamel*

Institute of Polymer Research, Department of Chemistry, University of Waterloo, Waterloo, ON N2L 3G1, Canada

Supporting Information

**ABSTRACT:** The molar absorbance coefficient of ground-state pyrene aggregates ($\varepsilon_{E0}(\lambda)$) in water generated by a short poly(ethylene oxide) chain labeled at a single end with a 1-pyrenemethoxide unit, namely, the polymeric construct $Py_1$-PEO(2.5K), was determined by a combination of UV−vis absorption and time-resolved fluorescence experiments. Since direct excitation of ground-state pyrene aggregates results in instantaneous excimer emission, whereas excimer formation by diffusive encounters between an excited- and a ground-state pyrene is delayed, acquisition of a pyrene monomer and excimer fluorescence decays with 1 nm increments of the excitation wavelength can probe the subtle effect that the excitation wavelength has on the extent of instantaneous excimer formation. These differences were taken advantage of to determine the fraction $f^{f}_{agg}(\lambda)$ of the total absorbance of the $Py_1$-PEO(2.5K) solution that is due to ground-state pyrene aggregates. This was achieved by fitting the pyrene monomer and excimer fluorescence decays globally with the model free analysis. For each wavelength, an $f^{f}_{agg}(\lambda)$ value was obtained which was then related to $\varepsilon_{E0}(\lambda)$ and $f_{agg}$, the molar fraction of aggregated pyrenes that is wavelength independent. These experiments were conducted for three $Py_1$-PEO(2.5K) concentrations yielding three similar $\varepsilon_{E0}(\lambda)$ spectra as expected since $\varepsilon_{E0}(\lambda)$ is an intrinsic property of the pyrene aggregates that should not depend on pyrene concentration. The $\varepsilon_{E0}(\lambda)$ spectra of the pyrene aggregates of $Py_1$-PEO(2.5K) in water were substantially broader and red-shifted compared to that of the pyrene monomer. Its measure provides a simple means to calculate the molar fraction of aggregated pyrene units in a $Py_1$-PEO(2.5K) aqueous solution from the absorption of the solution. This procedure should become widely applicable to determine $f_{agg}$ of water-soluble polymers which have been hydrophobically modified with a pyrene derivative and used as models for associative polymers.

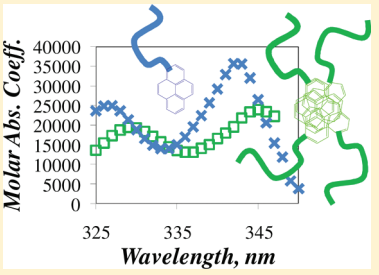


## INTRODUCTION

The low solubility of the chromophore pyrene in water and the changes undergone by its photophysical properties upon aggregation, particularly the ability for an excited pyrene to form an excimer upon complexation with a ground-state pyrene, make pyrene an ideal tool to probe the association of hydrophobically modified water-soluble polymers (HMWSPs).[1−4] HMWSPs are used in a variety of applications, as associative thickeners in paints,[5−8] shear-thinning agents for enhanced oil recovery,[9] drug delivery vehicles,[10] or colloidal stabilizers in cosmetics.[11] In a typical experiment, pyrene is covalently attached as the hydrophobe of the HMWSP to yield Py-HMWSP, and qualitative information about the level of association of the polymer is inferred from the strength of the pyrene−pyrene association obtained by monitoring the magnitude of the broadening of the absorption spectrum of pyrene, the shift between the fluorescence excitation spectra of the pyrene monomer and excimer, changes in the fluorescence intensity ratio between the pyrene excimer and monomer (the $I_E/I_M$ ratio), or the reduction in the rise time of the excimer decay.[1−4] These experiments are well-documented, and they have provided a wealth of information about the nature of HMWSP associations.

Considering the incredible amount of scientific attention garnered by pyrene aggregates over the years,[1−4] it might come as a surprise that the strength of pyrene aggregation is hardly ever described in terms of the molar fraction $f_{agg}$ of pyrene labels that are aggregated. This information is usually unavailable because the molar absorbance coefficient of a pyrene aggregate ($\varepsilon_{E0}(\lambda)$) is typically unknown. To this date, $\varepsilon_{E0}(\lambda)$ has been determined in a single instance, for the pyrene aggregates generated in the aqueous solution of water-soluble poly(*N*,*N*-dimethylacrylamide) randomly labeled with pyrene (Py-PDMA).[12]

The procedure outlined for the determination of $\varepsilon_{E0}(\lambda)$ in the case of Py-PDMA is based on a modified Birks' scheme[13] described in Scheme 1 where pyrene excimer formation occurs via two different routes, either via direct excitation of a ground-state pyrene dimer shown on the right or via excitation of a pyrene monomer followed by a diffusive encounter with a ground-state pyrene. Whereas direct excitation of a pyrene dimer results in instantaneous excimer formation, diffusion-controlled excimer formation occurs over time with a time-dependent rate constant $f(t)$. The function $f(t)$ was derived for Py-PDMA in water by noting that the diffusive encounters between pyrene labels randomly attached onto PDMA should be well-described by the Fluorescence Blob Model (FBM).[14,15]

**Received:** August 24, 2011
**Revised:** December 9, 2011
**Published:** January 23, 2012

**Scheme 1. Modified Birks' Scheme for Excimer Formation between Pyrene Pendants Attached onto a Polymer[a]**

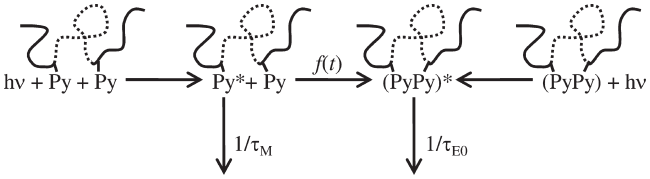


[a] Pyrene can be attached randomly onto the polymer (entire chain) or at one end (the central part of the chain with dashes disappears) resulting in intra- or intermolecular excimer formation, respectively.

The difference in the time taken to form an excimer is exploited to analyze the monomer and excimer fluorescence decays globally and retrieve $f^{f}_{agg}(\lambda)$ which represents the fraction of excitation light absorbed by aggregated pyrenes at the excitation wavelength $\lambda$. Mathematically, $f^{f}_{agg}(\lambda)$ equals $Abs_{Pyagg}(\lambda)/[Abs_{Pyagg}(\lambda) + Abs_{Pyn\text{-}agg}(\lambda)]$ where $Py_{agg}$ and $Py_{n\text{-}agg}$ represent the aggregated and nonaggregated pyrene species. The *f* superscript indicates that it is determined from the analysis of the fluorescence decays, and as a result, it is often referred to as a "fluorescence fraction". In turn, knowledge of the molar absorbance coefficient of the nonaggregated pyrene ($\varepsilon_M(\lambda)$) together with the overall pyrene concentration and absorbance of the Py-HMWSP solution allows one to use $f^{f}_{agg}(\lambda)$ to determine $\varepsilon_{E0}(\lambda)$ and the actual molar fraction of aggregated pyrenes ($f_{agg}(\lambda) = [Py_{agg}]/\{[Py_{agg}] + [Py_{n\text{-}agg}]\}$) at each wavelength. Since $f_{agg}$ is a measure of the level of pyrene association, it does not depend on wavelength. By acquiring the fluorescence decays of the pyrene monomer and excimer at different excitation wavelength, $\varepsilon_{E0}(\lambda)$ and $f_{agg}(\lambda)$ can be determined at these excitation wavelengths. The procedure is deemed valid if $f_{agg}(\lambda)$ is found to be independent of the excitation wavelength as its definition mandates. It was successfully applied to determine $\varepsilon_{E0}(\lambda)$ for pyrene aggregates generated by Py-PDMA constructs in water.[12]

This study provides a second $\varepsilon_{E0}(\lambda)$ spectrum for the pyrene aggregates formed in aqueous solutions of $Py_1$-PEO(2.5K), a poly(ethylene oxide) terminated at one end with a 1-pyrenemethoxide unit. The association of $Py_1$-PEO(2.5K) in aqueous solution has been fully characterized in an earlier publication where it was shown that $Py_1$-PEO(2.5K) self-assembles into polymeric micelles consisting of 20 $Py_1$-PEO(2.5K) units per micelle.[16] At a $Py_1$-PEO(2.5K) concentration larger than 10 $g \cdot L^{-1}$ equivalent to a molar concentration of 4 mmol $L^{-1}$, the polymeric micelles were found to aggregate into larger structures composed of individual $Py_1$-PEO(2.5K) micelles. The high local pyrene concentration inside a $Py_1$-PEO(2.5K) micelle allows for the formation of pyrene aggregates, and this study demonstrates that the fraction $f^{f}_{agg}$ can be determined by analyzing globally the pyrene monomer and excimer fluorescence decays according to Scheme 1. The different distributions of pyrene along the two polymeric backbones, pyrene being randomly attached onto PDMA in Py-PDMA[12] and at a single end of PEO in $Py_1$-PEO(2.5K),[16] imply that the FBM cannot be used to determine $f(t)$ in Scheme 1 for $Py_1$-PEO(2.5K) as was done with the Py-PDMA sample in reference 12. Instead, the recently developed Model Free (MF) analysis[17−19] was applied as it provides a general expression for $f(t)$ and thus enables the determination of the $\varepsilon_{E0}(\lambda)$ spectrum for the pyrene aggregates of Py-PDMA. Despite the different polymeric backbone of Py-PDMA and $Py_1$-PEO(2.5K), the $\varepsilon_{E0}(\lambda)$ spectra obtained for the pyrene aggregates generated by both pyrene-labeled polymeric constructs share several features which are discussed. Knowledge of $\varepsilon_{E0}(\lambda)$ for the pyrene aggregates generated by $Py_1$-PEO(2.5K) in water enables the quantitative determination of $f_{agg}$ for any aqueous solution of the many Py-HMWSPs which have been prepared to date with a poly(ethylene oxide) chain terminated at one end with a pyrene derivative.[12,16,17,20−41] It provides a new means of describing quantitatively the associative strength of these types of Py-HMWSPs via their $f_{agg}$ value.

## EXPERIMENTAL SECTION

**Materials.** The organic solvents hexanes (HPLC, Caledon), tetrahydrofuran (distilled in glass, Caledon), diethyl ether (GR ACS, EMD), methanol (HPLC, Caledon), and acetonitrile-190 (HPLC, Caledon) were used as received. All aqueous solutions were prepared with Milli-Q water with a resistivity of over 18 $M\Omega \cdot cm^{-1}$. Pyrene (98%, Aldrich) and 1-pyrenemethanol (98%, Aldrich) used in this study were both purified by three recrystallizations in methanol.

**Poly(ethylene oxide) Labeled at One End by Pyrene ($Py_1$-PEO(2.5K)).** $Py_1$-PEO(2.5K) was synthesized by DOW Chemical (Union Carbide division) following a procedure which has been described elsewhere.[16] $Py_1$-PEO(2.5K) was purified as follows. $Py_1$-PEO(2.5K) solutions in THF were precipitated three times with hexanes. The $Py_1$-PEO(2.5K) precipitate was dissolved in water, and it was washed three times against diethyl ether. $Py_1$-PEO(2.5K) was then dissolved in methanol at room temperature and allowed to cool in the refrigerator to 5 °C. The precipitated $Py_1$-PEO(2.5K) was filtered, and this step was repeated five times. The molecular weight of $Py_1$-PEO(2.5K) was determined to be 2500 g/mol by UV−vis absorption end-group analysis using the molar absorbance coefficient of 1-pyrenemethanol in tetrahydrofuran ($\varepsilon$(344 nm) = 42 700 $M^{-1}$ $cm^{-1}$). The polydispersity index of $Py_1$-PEO(2.5K) was determined to be 1.3 by gel permeation chromatography using a DRI detector.

**UV−vis Measurements.** A Beckman DU640 spectrophotometer was used for all absorbance measurements. All absorbance spectra were obtained with a spectral bandwidth resolution of 1 nm. To ensure linearity in the response of the spectrophotometer, cells with path lengths of 10, 1, and 0.1 mm were used to keep the absorbance signals between 0.05 and 2. The molar absorption coefficient of the unassociated $Py_1$-PEO(2.5K) in water was obtained by using a 2.5 $\mu$M solution of $Py_1$-PEO(2.5K) in water sufficiently dilute to ensure that the little contribution to the absorbance by pyrene aggregates was negligible.

**Steady-State Fluorescence Measurements.** Steady-state fluorescence spectra of pyrene were obtained using a Photon Technology International LS-100 steady-state fluorometer having a continuous Ushio UXL-75Xe xenon arc lamp and a PTI 814 photomultiplier detection system. The emission spectra were acquired by exciting the samples at 344 nm for $Py_1$-PEO(2.5K) solutions. At pyrene concentrations above 50 $\mu$M, the spectra were acquired using the front-face geometry.[42] The spectra acquired for concentrations of pyrene equal to or lower than 50 $\mu$M used a right-angle geometry.[42] All $Py_1$-PEO(2.5K) solutions in acetonitrile were bubbled under a gentle flow of $N_2$ gas for 40 min to remove molecularly dissolved oxygen. Residual solvent loss cannot be fully prevented with this procedure but never amounted to a weight loss greater than 5%.

Therefore, the concentrations reported in acetonitrile are slightly underestimated. All aqueous solutions were left aerated.

**Time-Resolved Fluorescence Measurements.** Fluorescence decays were acquired with an IBH Ltd. time-resolved fluorometer equipped with an IBH 340 nm NanoLED. For the concentration studies, all solutions of pyrene and 1-pyrenemethanol were excited at 338 and 344 nm, respectively. To determine $\varepsilon_{E0}(\lambda)$, the aqueous solutions of $Py_1$-PEO(2.5K) were excited at wavelengths in the range of 325−347 nm with one nanometer increments. To ensure a narrow excitation spectral bandwidth and hence a high resolution of $\varepsilon_{E0}(\lambda)$, the excitation monochromator slits were set with a bandwidth of 1 nm. The emission wavelength was set at 375 and 510 nm for the pyrene monomer and excimer decays, respectively. To reduce the noise stemming from stray scattered light, cutoff filters of 370 and 495 nm were used to acquire the monomer and excimer decays, respectively. Samples of $Py_1$-PEO(2.5K) in acetonitrile were degassed under a gentle flow of high purity nitrogen having a maximum impurity content of 4.8 ppm for 40 min to remove molecularly dissolved oxygen. All aqueous samples were left aerated. All decays were collected over 1024 channels with a minimum of 10 000 counts taken at the maximum of the monomer and excimer decays, respectively, to ensure a high signal-to-noise ratio. A light scattering suspension was used to obtain the profile of the lamp response. All measured decays were deconvoluted from the lamp profile and fitted to the desired function using a least-square analysis.[43] The resulting fits were characterized as "good" when the $\chi^2$ parameter was smaller than 1.3 and the residuals and the autocorrelation function of the residuals were randomly distributed around zero. The unquenched monomer lifetime, $\tau_M$, of pyrene, 1-pyrenemethanol, and $Py_1$-PEO(2.5K) in acetonitrile was found to equal 311, 253, and 279 ns, respectively. In aerated water, the pyrene monomer of $Py_1$-PEO(2.5K) had a lifetime of 155 ns. The monomer lifetime of $Py_1$-PEO(2.5K) was determined by fitting the monomer decay of a dilute $Py_1$-PEO(2.5K) solution to a biexponential function and taking the strongly contributing (95%) long decay time as $\tau_M$. The origin of the short decay time of $Py_1$-PEO(2.5K) in solution might be a result of residual interactions taking place between pyrene and the PEO backbone which leads to the undue quenching of a small fraction of the excited pyrene labels.

**Analysis of the Monomer and Excimer Fluorescence Decays.** The equations used to fit the monomer and excimer fluorescence decays according to Birks' scheme[13,20] or the MF analysis[17−19] have already been published in one form or another. They are given as, respectively, eqs S1 and S2 for Birks' Scheme and eqs S5 and S6 for the MF analysis in the Supporting Information (SI). The pyrene monomer and excimer fluorescence decays were fitted globally. Although eqs S1, S2, S5, and S6 are sums of exponentials similar to those typically found in the scientific literature to fit fluorescence decays,[21,44] the analysis of the pyrene monomer and excimer fluorescence decays carried out in the present study differs markedly from the current article, as the monomer and excimer decays are fitted globally with these equations by optimizing both the decay times *and* the pre-exponential factors with respect to the parameters describing the kinetics of excimer formation. As a number of reports from this laboratory have already demonstrated, this type of analysis enhances dramatically the accuracy of the parameters describing the kinetic Scheme 1.[18−20,45] Birks' Scheme and MF analysis of the fluorescence decays yielded good fits with randomly distributed residuals and autocorrelation function of the residuals, as well as $\chi^2$ that were all smaller than 1.30.

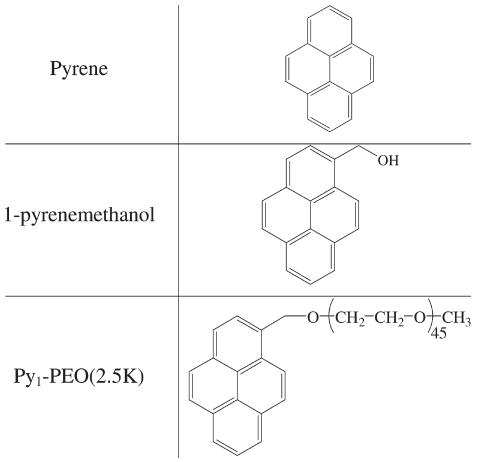


**Figure 1.** Chemical structures of pyrene, 1-pyrenemethanol, and $Py_1$-PEO(2.5K).

## RESULTS AND DISCUSSION

The sample under study is a poly(ethylene oxide) chain having a number-average molecular weight of 2500 g/mol labeled at one end with pyrene ($Py_1$-PEO(2.5K)) whose behavior in water has been the object of an in-depth study.[16] In water, the hydrophobic pyrene induces $Py_1$-PEO(2.5K) to self-assemble into polymeric micelles with a pyrene-rich core surrounded by a PEO corona. Pyrene aggregates are generated in the micellar core. To investigate the effect that pyrene aggregates would have on the MF analysis of the fluorescence decays, the kinetics of pyrene excimer formation were investigated for solutions of different pyrene derivatives, such as pyrene and 1-pyrenemethanol in acetonitrile, $Py_1$-PEO(2.5K) in acetonitrile where acetonitrile is a good solvent for both PEO and pyrene, and water, a specific solvent for the PEO block of $Py_1$-PEO(2.5K). The chemical structures of the different pyrene species used in this study are shown in Figure 1. The kinetics of pyrene excimer formation for pyrene and 1-pyrenemethanol in acetonitrile are considered first.

**Pyrene and 1-Pyrenemethanol in Acetonitrile.** Solutions were prepared with chromophore concentrations ranging from 0.2 to 10 mM. The monomer and excimer fluorescence decays were acquired and fitted according to Birks' scheme (i.e., eqs S1 and S2 in Supporting Information) and the MF analysis (eq S5 and S6 in Supporting Information). The fits were good, and the parameters retrieved from the fits are listed in Tables S1 and S2 (Supporting Information). Birks' scheme analysis yielded an excimer dissociation rate constant ($k_{-1}$) equal to 9.1 (±1.6) × $10^6$ $s^{-1}$ and 1.1 (±0.6) × $10^6$ $s^{-1}$ for pyrene and 1-pyrenemethanol, respectively.

Birks reports $k_{-1}$ values for pyrene in acetone (12 × $10^6$ $s^{-1}$) or ethanol (8.3 × $10^6$ $s^{-1}$) that are similar to the $k_{-1}$ value found in acetonitrile for pyrene.[13] The decrease of $k_{-1}$ by close to 1 order of magnitude for 1-pyrenemethanol suggests that the methanol functionality helps stabilize the excimer in acetonitrile. Pyrene and 1-pyrenemethanol had a similar excimer lifetime ($\tau_{E0}$) in acetonitrile equal to 50 (±6) and 50 (±2) ns, respectively. The product $k_1$ × [M] for excimer formation increased linearly with pyrene concentration, yielding identical rate constants $k_1$ equal to 11.1 (±0.1) × $10^9$ $M^{-1}$ $s^{-1}$ and 10.9 (±0.1) × $10^9$ $M^{-1}$ $s^{-1}$ for

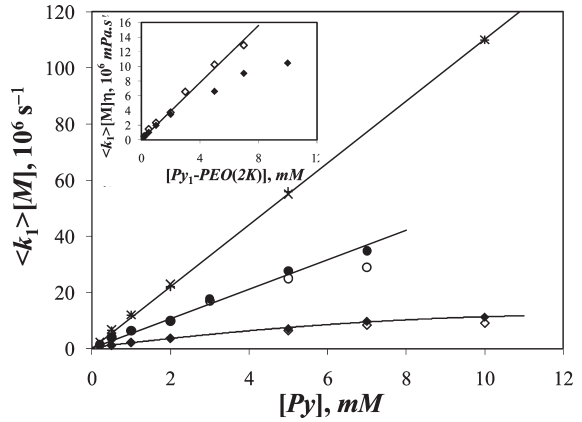


**Figure 2.** Viscosity uncorrected (hollow) and corrected (filled) product $<k_1> \times [M]$ for pyrene in acetonitrile (+), 1-pyrenemethanol in acetonitrile (×), $Py_1$-PEO(2.5K) in acetonitrile (●,○,), and $Py_1$-PEO(2.5K) in water (◆,◇). Inset: Product $<k_1> \times [M] \times \eta$ for $Py_1$-PEO(2.5K) in acetonitrile (◇) and water (◆).

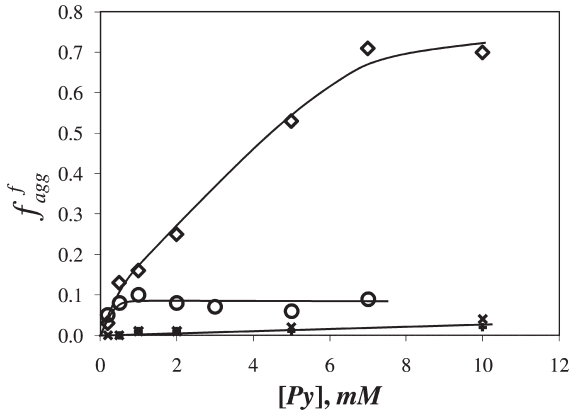


**Figure 3.** Plot of $f^f_{agg}$ as a function of pyrene concentration for pyrene in acetonitrile (+), 1-pyrenemethanol in acetonitrile (×), $Py_1$-PEO(2.5K) in acetonitrile (○), and $Py_1$-PEO(2.5K) in water (◇).

pyrene and 1-pyrenemethanol, respectively. As expected in an organic solvent where pyrene is soluble, hardly any pyrene aggregation could be detected. The fluorescence fraction of aggregated pyrenes ($f^f_{agg}(\lambda) = \varepsilon_{E0}(\lambda) \times [E0^*]_{(t=0)}/\{\varepsilon_{E0}(\lambda) \times [E0^*]_{(t=0)} + \varepsilon_M(\lambda) \times [Py_{diff}^*]_{(t=0)}\}$ where $[E0^*]_{(t=0)}$ and $[Py_{diff}^*]_{(t=0)}$ represent the concentrations of pyrenes that are aggregated and form an excimer by diffusion, respectively) equaled 0.003 (±0.002) and 0.02 (±0.02) for pyrene and 1-pyrenemethanol in acetonitrile, respectively. According to its definition, $f^f_{agg}(\lambda)$ depends on the excitation wavelength which was 338 and 344 nm for pyrene and 1-pyrenemethanol in acetonitrile, respectively.

Similar results were obtained with the MF analysis, and the parameters retrieved from this analysis are listed in Tables S3 and S4 (Supporting Information). The excimer lifetimes were found to equal 48 (±3) and 49 (±2) ns for pyrene and 1-pyrenemethanol, respectively. As shown in Figure 2, the product $<k_1> \times [M]$ given in eq S16 (Supporting Information) was found to increase linearly with increasing pyrene concentration (Figure 2). The average rate constant of excimer formation $<k_1>$ was found to equal 11.3 (±0.1) × $10^9$ $M^{-1}$ $s^{-1}$ and 11.0 (±0.1) × $10^9$ $M^{-1}$ $s^{-1}$ for pyrene and 1-pyrenemethanol, respectively. The fraction $f^f_{agg}$ shown in Figure 3 was also found to be rather small and equal to 0.01 (±0.01) and 0.01 (±0.02) for pyrene and 1-pyrenemethanol, respectively. This low level of aggregation is expected since acetonitrile is a good solvent for both chromophores. The results of these two analyses indicate that the rate constant of excimer formation and $\tau_{E0}$ for pyrene and 1-pyrenemethanol is identical, within experimental error, whether the fluorescence decays are fitted according to Birks' scheme or the MF analysis. It suggests that the MF analysis is an analytical tool that can probe intermolecular excimer formation as well as intramolecular excimer formation as was found earlier for various pyrene-labeled macromolecules.[17−19,45] It is now applied to study the kinetics of excimer formation for $Py_1$-PEO(2.5K) in acetonitrile and water.

**$Py_1$-PEO(2.5K) in Acetonitrile.** $Py_1$-PEO(2.5K) solutions with pyrene concentration ranging from 0.2 to 7 mM were prepared in acetonitrile. Their monomer and excimer fluorescence decays were acquired and fitted with eqs S5 and S6 (Supporting Information) according to the MF analysis. Since the fluorescence spectra of $Py_1$-PEO(2.5K) in acetonitrile showed very little excimer for $Py_1$-PEO(2.5K) concentrations smaller than 0.2 mM, the MF analysis of the fluorescence decays was carried out for those $Py_1$-PEO(2.5K) concentrations larger than 0.2 mM. The diffusive encounters between two pyrene moieties covalently attached to a single end of a chain are described by a time-dependent rate constant.[46] Within the framework of the MF analysis, it implies that more than one exponential in eq S5 (Supporting Information) is needed to fit the monomer decays, as found experimentally as two exponentials ($n$ = 2 in eq S5, Supporting Information) were needed to fit the monomer decays. The analysis of the excimer decays assumed the presence of short-lived pyrene dimers $ES^*$ having a lifetime of 3.5 ns. This lifetime of 3.5 ns was fixed in the analysis, and it was obtained by averaging the values of the short decay time obtained from the fit of the excimer decays of the $Py_1$-PEO(2.5K) solutions in acetonitrile with a sum of exponentials. A lifetime of 3.5 ns is close to the $\tau_{ES}$ values obtained for other pyrene-labeled macromolecules forming short-lived ground-state pyrene dimers $ES^*$.[21,47,48] Although small, the contribution from the short-lived fluorescent species needed to be accounted for to obtain good fits. The analysis of the fluorescence decays was found to be fairly insensitive to the exact value of $\tau_{ES}$ as changing its value from 3.5 to 2.5 or 4.5 ns resulted in a change in the fluorescence fractions that was smaller than 4%.

The parameters obtained from the fits are listed in Table S5 (Supporting Information). The contribution of $ES^*$ to the fluorescence decays given by $f^f_{ES}$ was small. Together, the contributions of $ES^*$ and $E0^*$ given by $f^f_{agg} = f^f_{ES} + f^f_{E0}$ amounted to less than 10% for all $Py_1$-PEO(2.5K) concentrations so that $Py_1$-PEO(2.5K) can be considered to be unaggregated in acetonitrile up to a concentration of 7 mM (Figure 3). The excimer lifetime remained constant within experimental error and equal to 52 ± 8 ns. This value is similar to those found for pyrene and 1-pyrenemethanol in acetonitrile. Contrary to pyrene and 1-pyrenemethanol, the product $<k_1> \times [M]$ did not increase linearly with $Py_1$-PEO(2.5K) concentration but showed a downward curvature with increasing polymer concentration in Figure 2. Since concentrations of $Py_1$-PEO(2.5K) as high as 5−10 mM have an effect on the solution viscosity $\eta$ that is much more significant than 5−10 mM pyrene or 1-pyrenemethanol, the product $<k_1> \times [M]$ might be affected by an increase in the solution viscosity.

Thus, the viscosity of $Py_1$-PEO(2.5K) solutions was determined in the same concentration range as that used in Figure 2

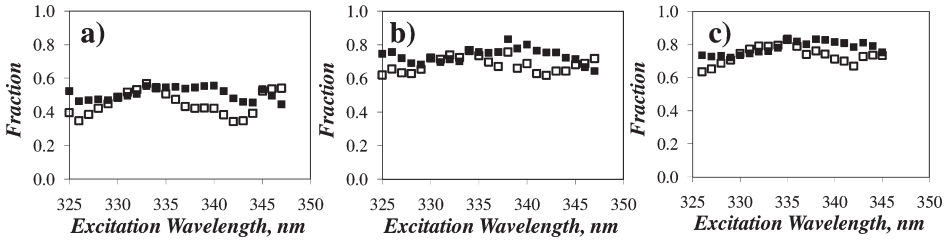


**Figure 4.** Actual (filled) and fluorescence (hollow) fractions of aggregated pyrenes for aqueous solutions of $Py_1$-PEO(2.5K) having concentrations of (a) 5, (b) 10, and (c) 13 mM.

(see Table S6 in SI). It was found that the solution viscosity increased by 20% for the highest $Py_1$-PEO(2.5K) concentration used of 7 mM. Since the rate constant of excimer formation by diffusion is expected to be inversely proportional to the solution viscosity, $\langle k_1 \rangle \times [M]$ was multiplied by the ratio $\eta/\eta_0$ where $\eta$ and $\eta_0$ are, respectively, the viscosities of the solution and solvent at 25 °C. A plot of $\langle k_1 \rangle \times [M] \times (\eta/\eta_0)$ versus polymer concentration yielded a linear trend in Figure 2 with a $\langle k_1 \rangle \eta/\eta_0$ value of $5.0 \pm 0.2 \times 10^9\ M^{-1}\ s^{-1}$. This value is half that found for pyrene and 1-pyrenemethanol in acetonitrile as determined experimentally. This result is reasonable since the smaller $\langle k_1 \rangle \eta/\eta_0$ value reflects the slower kinetics of excimer formation experienced by the bulkier $Py_1$-PEO(2.5K) in acetonitrile.

**$Py_1$-PEO(2.5K) in Water.** The MF analysis was applied to the monomer and excimer fluorescence decays acquired for aqueous solutions of $Py_1$-PEO(2.5K) with concentrations between 0.2 and 10 mM to determine the fluorescence fractions of the pyrene species present in solution. As was the case for $Py_1$-PEO(2.5K) in acetonitrile, it was necessary to include a short-lived species having a lifetime of 3.5 ns to fit the excimer decays. Its contribution was found to be important at $Py_1$-PEO(2.5K) concentrations greater than 1 mM. The parameters obtained from the model free analysis of the monomer and excimer decays acquired for $Py_1$-PEO(2.5K) solutions in water are listed in Table S8 (Supporting Information). Significant differences were found between the trends obtained with the parameters $\langle k_1 \rangle \times [M]$ and $f^f_{agg}$ in solutions of $Py_1$-PEO(2.5K) in water and acetonitrile. While $f^f_{agg}$ was less than 10% and essentially independent of $Py_1$-PEO(2.5K) concentration in acetonitrile, $f^f_{agg}$ in water increased to values as high as 0.70 within the same $Py_1$-PEO(2.5K) concentration range (Figure 3). Furthermore, whereas multiplying $\langle k_1 \rangle \times [M]$ by $\eta/\eta_0$ resulted in a linear increase with increasing $Py_1$-PEO(2.5K) concentration in acetonitrile, the same was not observed in water as shown in Figure 2 where $\langle k_1 \rangle \times [M] \times \eta/\eta_0$ deviates from linearity for $Py_1$-PEO(2.5K) concentrations greater than 2 mM. Incidentally, it is in this concentration range that $f^f_{agg}$ takes larger values. This coincidence suggests that the aggregation of $Py_1$-PEO(2.5K) is likely the cause of the deviation. This point is further supported by plotting the product $\langle k_1 \rangle \times [M] \times \eta$ as a function of $Py_1$-PEO(2.5K) concentration in the inset of Figure 2. At low polymer concentration ($[Py_1\text{-PEO(2.5K)}] < 2$ mM) where $f^f_{agg}$ is small ($f^f_{agg} < 0.25$), the products $\langle k_1 \rangle \times [M] \times \eta$ obtained in acetonitrile and water are the same. At higher $Py_1$-PEO(2.5K) concentration, where $f^f_{agg}$ is large, the trends obtained for $\langle k_1 \rangle \times [M] \times \eta$ in water and acetonitrile depart from one another. For large $f^f_{agg}$ values, the pyrene groups of $Py_1$-PEO(2.5K) are not homogeneously distributed in the solution. The effective concentration of pyrene groups that can undergo excimer formation via translational diffusion through the solution is actually smaller than the total pyrene concentration resulting in a downward curvature when the product $\langle k_1 \rangle \times [M]$ is plotted as a function of the total pyrene concentration in Figure 2.

Although the plot of $\langle k_1 \rangle \times [M] \times (\eta/\eta_0)$ against $Py_1$-PEO(2.5K) concentration in water shows a substantial degree of curvature, the ratio $I_E/I_M$ of the intensities of the excimer ($I_E$), integrated from the fluorescence emission spectra between 500 and 530 nm, to that of the monomer ($I_M$), integrated from the fluorescence emission spectra between 372 and 378 nm, has been shown to exhibit a linear relationship with $Py_1$-PEO(2.5K) concentration in water.[16] The $I_E/I_M$ ratio, being referred to as the "coiling index",[3] is a common approach to the characterization of pyrene-labeled polymers in solution. The coiling index is often considered to represent the same effect as $\langle k_1 \rangle \times [M]$. For Py-HMWSPs such as $Py_1$-PEO(2.5K), however, this does not appear to be true since the quantity $\langle k_1 \rangle \times [M] \times \eta/\eta_0$ in water was observed to plateau in Figure 2, whereas $I_E/I_M$ exhibits a linear dependence with $Py_1$-PEO(2.5K) concentration.[16] Since $\langle k_1 \rangle \times [M] \times \eta/\eta_0$ accounts only for diffusionally formed excimers while $I_E/I_M$ includes both excimers generated by the direct excitation of GS pyrene aggregates and by diffusive encounters of pyrene monomers, differences in the trends of $\langle k_1 \rangle \times [M] \times \eta/\eta_0$ and $I_E/I_M$ are expected for this particular case.

The results on pyrene excimer formation suggest that the MF analysis can be used to characterize the kinetics of excimer formation by diffusion. Furthermore, the MF analysis seems to respond to the presence of GS pyrene aggregates formed by $Py_1$-PEO(2.5K) in water, as $f^f_{agg}$ was found to increase with increasing $Py_1$-PEO(2.5K) concentration in Figure 3. Consequently, the MF analysis appears to be an alternate analytical tool to the FBM to describe the kinetics of excimer formation of a pyrene-labeled polymer and its level of pyrene association $f^f_{agg}$ as was already demonstrated in at least one occasion.[17] These considerations lead to the conclusion that the MF analysis can be applied to determine the molar absorbance coefficient of the pyrene aggregates formed by $Py_1$-PEO(2.5K) in water. This recommendation is being implemented in the following section.

**Molar Absorption Coefficient of Pyrene Aggregates.** The monomer and excimer fluorescence decays of 5, 10, and 13 mM solutions of $Py_1$-PEO(2.5K) in water were acquired using excitation wavelengths ranging from 325 to 347 nm with 1 nm increments and 1 nm slit width on the excitation monochromator to ensure high spectral resolution. These three $Py_1$-PEO(2.5K) concentrations were selected since their solution undergoes substantial pyrene aggregation as they display sufficient broadening of their absorption spectra compared to the 2 $\mu$M solution of unassociated $Py_1$-PEO(2.5K) in water. Indeed, their $P_A$ values, defined as the ratio of the maximum absorption to that of the nearest trough, for 5, 10, and 13 mM $Py_1$-PEO(2.5K) solutions, were found to equal 2.1, 1.8, and 1.7, respectively. These $P_A$

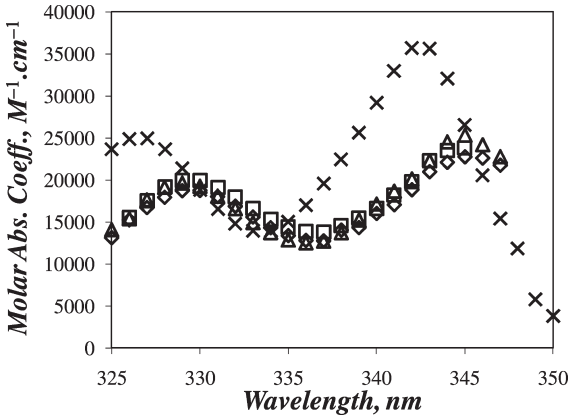


**Figure 5.** Molar absorbance coefficients of unassociated $Py_1$-PEO(2.5K) in water (×) and pyrene aggregates determined for $Py_1$-PEO(2.5K) solutions in water of 5 (Δ), 10 (◇), and 13 (□) mM.

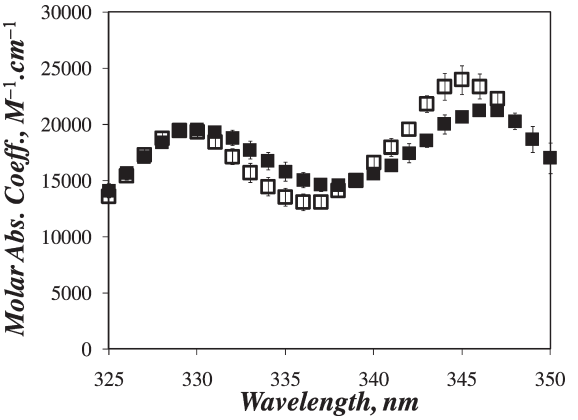


**Figure 6.** Averaged molar absorbance coefficients of pyrenes that are aggregated, $<\varepsilon_{E0}>$, determined for $Py_1$-PEO(2.5K) (□) and Py-PDMA (■) in water.

values indicate considerable broadening of their absorption spectra compared to the 2 $\mu$M $Py_1$-PEO(2.5K) solution which was found to have a $P_A$ value of 2.6. Since the level of aggregation of a pyrene-labeled macromolecule is reflected by a $P_A$ value much smaller than 3.0, the 2 $\mu$M $Py_1$-PEO(2.5K) solution in water is substantially less aggregated than the three other solutions. The monomer and excimer decays at each excitation wavelength were fitted globally with the MF approach, and the obtained parameters are listed in Tables S9−S11 (Supporting Information). As was observed for the pyrene aggregates of Py-PDMA,[12] the fluorescence fraction $f^f_{agg}(\lambda)$ exhibits substantial excitation wavelength dependency in Figure 4. The calculated molar fraction of aggregated pyrenes $f_{agg}$ exhibits a smaller excitation wavelength dependency compared to $f^f_{agg}(\lambda)$ as the undulations in Figure 4 are less pronounced and less patterned for $f_{agg}$. On the basis of the trends shown in Figure 4, $f_{agg}$ increases with increasing $Py_1$-PEO(2.5K) concentration, being equal to 0.51 ± 0.04, 0.74 ± 0.04, and 0.78 ± 0.04 for aqueous $Py_1$-PEO(2.5K) solutions of 5, 10, and 13 mM, respectively.

In addition to $f_{agg}$, the molar absorbance coefficient of the pyrene aggregates $\varepsilon_{E0}(\lambda)$ was also calculated for each of the three $Py_1$-PEO(2.5K) concentrations. The three sets of molar absorbance coefficients are shown in Figure 5 along with the molar absorbance coefficient of unassociated $Py_1$-PEO(2.5K). The molar absorbance coefficient spectra of the aggregated species, with an average $P_A$ value equal to 1.8 ± 0.1, exhibit much broader and smaller peaks compared to the unassociated species. The absorption maximum at 342.5 nm for the pyrene monomer is red-shifted to 345 nm for the pyrene aggregates. Both broadening and red-shift of the absorbance spectrum are features that are expected when comparing the absorbance spectrum of aggregated pyrenes with that of the pyrene monomer.[1−4] Despite the differences in $f_{agg}$ between the three concentrations, there is good agreement between the three sets of $\varepsilon_{E0}(\lambda)$ values determined for the three $Py_1$-PEO(2.5K) concentrations. This agreement suggests that the procedure used to determine $\varepsilon_{E0}(\lambda)$ introduced 3 years ago to determine the molar absorbance coefficient of the pyrene aggregates of Py-PDMA and outlined in the Supporting Information is valid and was successfully applied to the pyrene aggregates of $Py_1$-PEO(2.5K) in water.

The molar absorbance coefficients for the pyrene aggregates obtained for the three $Py_1$-PEO(2.5K) concentrations between 325 and 347 nm were averaged, and the average value $<\varepsilon_{E0}>$ is listed in Table S13 (Supporting Information) as a function of wavelength. The $\varepsilon_{E0}(\lambda)$ spectrum of $Py_1$-PEO(2.5K) was compared to that of the Py-PDMA samples[12] in Figure 6. The $\varepsilon_{E0}(\lambda)$ spectra of $Py_1$-PEO(2.5K) and Py-PDMA exhibit similar features, being broader and red-shifted compared to the $\varepsilon_M(\lambda)$ spectrum of the pyrene monomer, but the $\varepsilon_{E0}(\lambda)$ spectrum of Py-PDMA in water is broader and more red-shifted than that of $Py_1$-PEO(2.5K). Such differences are not entirely unexpected since the pyrene aggregates of Py-PDMA and $Py_1$-PEO(2.5K) have certainly different composition that will affect the interactions between the chromophores leading to changes in the balance between well- and poorly stacked pyrene dimers. The present analysis makes the assumption that $\varepsilon_{ES}(\lambda)$ equals $\varepsilon_{E0}(\lambda)$. Thus, the $\varepsilon_{E0}(\lambda)$ values reported in Figure 6 represent average values of the molar absorbance coefficient of the pyrene aggregates present in solution. Although our current treatment of the data does not allow us to distinguish between $\varepsilon_{ES}(\lambda)$ and $\varepsilon_{E0}(\lambda)$, the differences in the trends shown in Figure 6 suggest that well- and poorly stacked pyrene dimers might not have the same molar absorbance coefficient.

As a short PEO chain terminated at one end by a hydrophobe (HP-PEO), the $Py_1$-PEO(2.5K) construct constitutes a polymeric model that is an essential building block of two major families of associative thickeners used commercially, namely, the HASE (hydrophobically modified alkali swellable emulsion copolymer) and HEUR (hydrophobically modified ethoxylated urethane polymer) families.[49] The peculiar viscoelastic properties exhibited by HASE and HEUR aqueous solutions are due to the associations of the hydrophobes of HP-PEO segments located either randomly along the chain or at the ends, respectively. The $\varepsilon_{E0}(\lambda)$ spectrum obtained for the pyrene aggregates of $Py_1$-PEO(2.5K) enables the determination of the level of association of aqueous solutions of pyrene-labeled HASE or HEUR in terms of their $f_{agg}$ value. For instance, $f^f_{agg}$ was found to equal 0.07 for a doubly end-labeled PEO ($Py_2$-PEO(8K)) upon excitation at 342 nm.[23] Using a molar absorbance coefficient of 36 000 and 19 600 $M^{-1}$ $cm^{-1}$ for the pyrene monomer (see Table S12, Supporting Information) and aggregates, an $f_{agg}$ value of 0.12 is retrieved indicating that 88 mol % of the pyrene units are not aggregated in $10^{-6}$ M solution of $Py_2$-PEO(8K).

Similarly, $f^f_{agg}$ values of 0.66 and 0.52 were measured at 344 nm for polymer concentrations ranging from 0.05 to 20 g $L^{-1}$ for two pyrene-labeled HASE samples with pyrene contents of 42

(Py-HASE(42)) and 65 (Py-HASE(65)) $\mu$mol g$^{-1}$, respectively.[23] Using values of $\varepsilon_M(\lambda)$ in Table S12 (Supporting Information) and $\varepsilon_{E0}(\lambda)$ in Table S13 (Supporting Information) of 32 000 and 23 400 M$^{-1}$ cm$^{-1}$ for the pyrene monomer and aggregates at 344 nm, $f_{agg}$ values of 0.73 and 0.60 are found for Py-HASE(42) and Py-HASE(65), indicating much stronger pyrene−pyrene associations for the Py-HASE samples than for the $Py_2$-PEO(8K) sample. Thanks to the $\varepsilon_{E0}(\lambda)$ values reported in Table S13 (Supporting Information), the $f_{agg}$ value of Py-HMWSP can now be determined in aqueous solution for the numerous Py-HMWSPs that contain the structural motif $Py_1$-PEO and which have been described in the scientific literature.[12,16,17,20−41] Since $f_{agg}$ is related to the ability of HMWSPs to form transient interpolymeric networks resulting in intriguing viscoelastic properties, the experiments carried out in the present study bear the promise that the effect that $f_{agg}$ has on the viscoelastic properties of solutions of Py-HMWSPs can now be investigated in a quantitative manner.

## CONCLUSIONS

The networking ability of the commercially available HASE and HEUR associative polymers is based in both cases on the aggregation of poly(ethylene oxide) chains end-capped with a hydrophobic moiety. To gain information on the level of association of these polymers, a model poly(ethylene oxide) chain capped at one end with a pyrene moiety ($Py_1$-PEO(2.5K)) was studied using a model free global analysis. The model free (MF) global analysis was first applied to study excimer formation of pyrene and 1-pyrenemethanol in acetonitrile, and the kinetic parameters retrieved from their analysis were compared to those obtained with the well-established Birks' scheme. The fact that analysis of the fluorescence decays with the MF approach or the well-established Birks' scheme yielded comparable kinetic parameters was taken as a validation of the MF analysis to study the intermolecular formation of the pyrene excimer. The MF approach was also used to determine the fluorescence fraction $f^f_{agg}$ of $Py_1$-PEO(2.5K) in solvents where $Py_1$-PEO(2.5K) was unassociated (acetonitrile) and associated into micelles (water). The MF global analysis was found to effectively characterize the fractions of each pyrene species to the decays, even for the difficult case of $Py_1$-PEO(2.5K) in water whose lack of rise time in the excimer decays could have prevented successful analysis of the decays. With the fluorescence fractions determined for $Py_1$-PEO(2.5K) in water, the true level of association $f_{agg}$ was characterized for three concentrations of $Py_1$-PEO(2.5K) in water and resulted also in the determination of one of the only two molar absorbance coefficient spectra $\varepsilon_{E0}(\lambda)$ of aggregated pyrenes available in the scientific literature today, namely, the one of $Py_1$-PEO(2.5K) and Py-PDMA. The $\varepsilon_{E0}(\lambda)$ spectrum obtained for Py-PDMA was broader and red-shifted compared to the $\varepsilon_{E0}(\lambda)$ spectrum obtained for $Py_1$-PEO(2.5K). The difference in the absorption spectra was attributed to differences in the nature of the pyrene dimers that constituted the pyrene aggregates, being partly long- and short-lived for the pyrene aggregates of Py-PDMA and $Py_1$-PEO(2.5K), respectively. This study confirms the flexibility and robustness of the MF analysis which can describe quantitatively the complex kinetics of pyrene excimer formation whether it takes place intra- or intermolecularly.

## ASSOCIATED CONTENT

**Supporting Information.** Derivations of equations used to fit the fluorescence decays according to Birks' scheme and the Model Free analysis; tables listing the kinetic parameters retrieved from the analysis of the fluorescence decays of pyrene, 1-pyrenemethanol, and $Py_1$-PEO(2.5K) in acetonitrile and water; tables listing the viscosity of $Py_1$-PEO(2.5K) solutions in acetonitrile and water. Tables listing the molar extinction coefficient of the pyrene aggregates of $Py_1$-PEO(2.5K) in water. This material is available free of charge via the Internet at http://pubs.acs.org.

## ACKNOWLEDGMENT

The authors thank NSERC and the ACS Petroleum Research Fund for financial support.

## REFERENCES

(1) Winnik, F. M. *Chem. Rev.* **1993**, *93*, 587–614.
(2) Winnik, F. M.; Regismond, S. T. A. *Colloids Surf., A* **1996**, *118*, 1–39.
(3) Duhamel, J. *Molecular Interfacial Phenomena of Polymers and Biopolymers*; Chen, P., Ed.; Woodhead: New York, 2005; pp 214−248.
(4) Pina, J.; Costa, T.; Seixas de Melo, J. S. *Photochemistry* **2011**, *38*, 67–109.
(5) *Polymers in Aqueous Media: Performance through Association*; Glass, J. E., Ed.; ACS Advances in Chemistry Series 223; ACS: Washington DC, 1989.
(6) *Hydrophilic Polymers: Performance with Environmental Acceptance*; Glass, J. E., Ed.; ACS Advances in Chemistry Series 248; ACS: Washington DC, 1996.
(7) *Associative Polymers in Aqueous Media*; Glass, J. E., Ed.; ACS Advances in Chemistry Series 765; ACS: Washington DC, 2000.
(8) Winnik, M. A.; Yekta, A. *Curr. Opin. Colloid Interface Sci.* **1997**, *2*, 424–436.
(9) Taylor, K. C.; Hawkins, B. F. In *Emulsions Fundamentals and Applications in the Petroleum Industry*; Schramm, L. L., Ed.; ACS Advances in Chemistry Series 231; ACS: Washington DC, 1992; pp 263−293.
(10) Duncan, R. *Nat. Rev. Drug Discovery* **2003**, *2*, 347–360.
(11) Lockhead, R. Y. In *Cosmetic Nanotechnology: Polymers and Colloids in Cosmetics*; ACS Symposium Series; ACS: Washington DC, 2007; pp 3−56.
(12) Siu, H.; Duhamel, J. *J. Phys. Chem. B* **2008**, *112*, 15301–15312.
(13) Birks, J. B. *Photophysics of Aromatic Molecules*; Wiley: New York, 1970; p 351.
(14) Mathew, H.; Siu, H.; Duhamel, J. *Macromolecules* **1999**, *32*, 7100–7108.
(15) Duhamel, J. *Acc. Chem. Res.* **2006**, *39*, 953–960.
(16) Siu, H.; Prazeres, T. J. V.; Duhamel, J.; Olesen, K.; Shay, G. *Macromolecules* **2005**, *38*, 2865–2875.
(17) Siu, H.; Duhamel, J. *J. Phys. Chem. B* **2005**, *109*, 1770–1780.
(18) Yip, J.; Duhamel, J.; Bahun, G.; Adronov, A. *J. Phys. Chem. B* **2010**, *114*, 10254–10265.
(19) Keyes-Baig, C.; Duhamel, J.; Wettig, S. *Langmuir* **2011**, *27*, 3361–3371.
(20) Chen, S.; Duhamel, J.; Winnik, M. A. *J. Phys. Chem. B* **2011**, *115*, 3289–3302.
(21) Costa, T.; Seixas de Melo, J.; Burrows, H. D. *J. Phys. Chem. B* **2009**, *113*, 618–626.
(22) Duhamel, J.; Yekta, A.; Hu, Y.; Winnik, M. A. *Macromolecules* **1992**, *25*, 7024–7030.
(23) Prazeres, T. J. V.; Beingessner, R.; Duhamel, J.; Olesen, K.; Shay, G.; Bassett, D. R. *Macromolecules* **2001**, *34*, 7876–7884.
(24) Ghiggino, K. P.; Snare, M. J.; Thistlethwaite, P. J. *Eur. Polym. J.* **1985**, *21*, 265–272.

(25) Cheung, S.-T.; Winnik, M. A.; Redpath, A. E. C. *Makromol. Chem.* **1982**, *183*, 1815–1824.
(26) Lee, S.; Winnik, M. A. *Macromolecules* **1997**, *30*, 2633–2641.
(27) Lee, S.; Duhamel, J. *Macromolecules* **1998**, *31*, 9193–9200.
(28) Farinha, J. P. S; Piçarra, S.; Miesel, K.; Martinho, J. M. G. *J. Phys. Chem. B* **2001**, *105*, 10536–10545.
(29) Cuniberti, C.; Perico, A. *Eur. Polym. J.* **1977**, *13*, 369–374.
(30) Char, K.; Frank, C. W.; Gast, A. P.; Tang, W. T. *Macromolecules* **1987**, *20*, 1833–1838.
(31) Char, K.; Gast, A.; Frank, C. W. *Langmuir* **1988**, *4*, 989–998.
(32) Char, K.; Frank, C. W.; Gast, A. P. *Macromolecules* **1989**, *22*, 3177–3180.
(33) Char, K.; Frank, C. W.; Gast, A. P. *Langmuir* **1989**, *5*, 1335–1340.
(34) Quina, F.; Abuin, E.; Lissi, E. *Macromolecules* **1990**, *23*, 5173–5175.
(35) Richey, B.; Kirk, A. B.; Eisenhart, E. K.; Fitzwater, S.; Hook, J. *J. Coat. Technol.* **1991**, *63*, 31–40.
(36) Eckert, A. R.; Hsiao, J.-S.; Webber, S. E. *J. Phys. Chem.* **1994**, *98*, 12025–12031.
(37) Abuin, E.; Lissi, E. *Eur. Polym. J.* **1992**, *28*, 125–127.
(38) Hu, Y.-Z.; Zhao, C.-L.; Winnik, M. A.; Sundarajan, P. R. *Langmuir* **1990**, *8*, 880–883.
(39) Maltesh, C.; Somasundaran, P. *Langmuir* **1992**, *8*, 1926–1930.
(40) Haldar, B.; Mallick, A.; Chattopadhyay, N. *J. Mol. Liq.* **2004**, *115*, 113–120.
(41) Haldar, B.; Chakrabarty, A.; Mallick, A.; Mandal, M. C.; Das, P.; Cattopadhyay, N. *Langmuir* **2006**, *22*, 3514–3520.
(42) Lakowicz, J. R. *Principles of Fluorescence Spectroscopy*; Plenum Press: New York, 1983; pp 43—47.
(43) Press, W. H.; Flannery, B. P.; Teukolsky, S. A.; Vetterling, W. T. *Numerical Recipes. The Art of Scientific Computing (Fortran Version)*; Cambridge University Press: Cambridge, 1992.
(44) Maçanita, A. L.; Zachariasse, K. A. *J. Phys. Chem. A* **2011**, *115*, 3183–3195.
(45) Chen, S.; Duhamel, J.; Bahun, G.; Adronov, A. *J. Phys. Chem. B* **2011**, *115*, 9921–9929.
(46) Martinho, J. M. G.; Campos, M.; Tencer, M.; Winnik, M. A. *Macromolecules* **1987**, *20*, 1582–1587.
(47) Siu, H.; Duhamel, J.; Sasaki, D.; Pincus, J. L. *Langmuir* **2010**, *26*, 10985–10994.
(48) Piçarra, S.; Gomes, P. T.; Martinho, J. M. G. *Macromolecules* **2000**, *33*, 3947–3950.
(49) Lundberg, D. J.; Glass, J. E.; Eley, R. R. *J. Rheol.* **1991**, *35*, 1255–1274.